Generation of Cherenkov superradiance pulses with a peak power exceeding the power of the driving short electron beam

S. D. Korovin, A. A. Eltchaninov, and V. V. Rostov
Institute of High Current Electronics, Russian Academy of Sciences, Tomsk, Russia

V. G. Shpak and M. I. Yalandin
Institute of Electrophysics, Russian Academy of Sciences, Ekaterinburg, Russia

N. S. Ginzburg, A. S. Sergeev, and I. V. Zotova
Institute of Applied Physics, Russian Academy of Sciences, Nizhny Novgorod, Russia
(Received 26 February 2006; published 6 July 2006)

Theoretical investigation of a short electron beam (extended bunch) interaction with a backward wave propagating in a slow wave structure demonstrates the possibility of producing ultrashort superradiance pulses with a peak power which exceeds the power of the driving beam (conversion factor $K>1$). It is shown that a nonuniform slow wave structure with optimized profile is beneficial in order to increase the conversion factor. The results of theoretical analysis are confirmed by the experiments. At *X* band using the SINUS-150 accelerator (4 ns, 330 kV, 2.6 kA) 0.6–0.8 ns superradiance pulses with a peak power of 1.2 GW and a conversion factor of 1.5 were obtained. Similar experiments at Ka-band based on the RADAN-303 accelerator (1 ns, 290 kV, 2.5 kA) demonstrated production of the superradiance (SR) pulse with duration 200 ps and peak power about 1 GW (conversion factor of 1.4).

DOI: 10.1103/PhysRevE.74.016501 PACS number(s): 41.60.Bq, 42.50.Fx, 07.57.Hm

I. INTRODUCTION

One of the main characteristics of traditional microwave oscillators and amplifiers driven by quasicontinuous electron beams is the efficiency defined as a ratio of the radiation power and power of the driving electron beam. The challenge of enhancing the efficiency is one of the key problems in microwave electronics. However, in all microwave devices operating in the steady state regime the efficiency is less than 1. At the same time this restriction is not applied in the case of a nonstationary electron-wave interaction and in such a case the radiation power can exceed the power of the electron beam. In Ref. [1] this fact was demonstrated for the amplification of a short incident electromagnetic pulse propagating through a long electron beam. If the electromagnetic pulse group velocity varied from the electron longitudinal velocity, the process of pulse amplification is significantly different from the well-known mechanism for monochromatic continuous signal amplification. Due to the propagation of the electromagnetic pulse along the electron beam, the front of this pulse is effectively amplified by unperturbed parts of the electron beam. As a result after some propagation distance the peak power of amplified pulse can exceed the power of electron beam. Obviously this conclusion does not contradict the energy conservation law because the full energy of the electromagnetic pulse is still smaller than the total energy of the beam.

In this paper we study the possibilities to generate electromagnetic pulses with the peak power exceeding the driving electron beam power using the process of superradiative emission. For classical electronics we understand superradiance (SR) as the coherent electromagnetic emission in the short single pulse from a moving extended electron bunch in the absence of an incident wave and any external feedback [2–15]. The coherence of the radiation is caused by a self-bunching effect inside the electron ensemble and the slippage of the electromagnetic wave with respect to electrons due to the difference between the electromagnetic wave group velocity and the electron longitudinal velocity. The superradiance can be obtained for various mechanisms of stimulated emission: cyclotron, Cherenkov, bremsstrahlung, etc. All the above types of SR were recently observed experimentally at millimeter and centimeter wavelength bands [9–15]. At the present stage the SR pulses with the highest peak power are obtained for the Cherenkov mechanism for the case when the electrons interact with synchronous harmonics of the backward wave propagating in slow wave structures (SWS).

Below, the detailed theory of the Cherenkov superradiance into a backward propagating wave is presented. It is shown that the optimization of the SWS parameters provides the conditions for the generation of the superradiance pulses with a peak power exceeding the power of the driving short electron beam (extended bunch). The theoretical results are confirmed by several series of experiments on production of ultrashort high power microwave pulses at Ka and X-band frequencies. In Sec. I a basic model is described in the frame of the averaged nonstationary approach. In Sec. II we study the Cherenkov SR in the uniform slow-wave structure. The conditions are found when the peak power of the electromagnetic pulse is proportional to the square of the total number of particles in the electron bunch, which is a specific feature of superradiance. In Sec. III it is shown that using a nonuniform SWS with an optimized impedance profile, the conversion coefficient (the ratio of the SR pulse peak power to the electron bunch power), can significantly exceed 1. In Sec. IV the experiments on production of Ka- and X-bands SR pulses with a peak power exceeding the power of the driving beam are described. All experiments are accompanied with direct particle-in-cell (PIC) code simulations, which include both the bunch formation and the radiation processes.

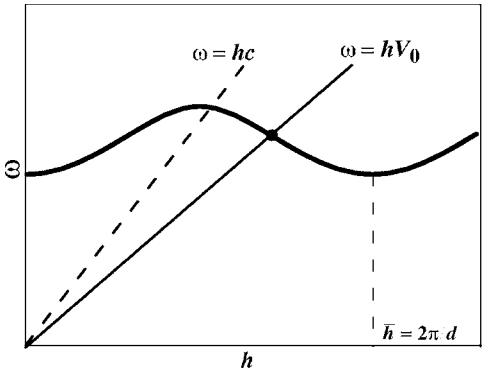

FIG. 1. Dispersion diagram for Cherenkov interaction of electrons with a spatial harmonic of backward wave in a periodically corrugated waveguide.

II. BASIC MODEL

Let us consider the stimulated Cherenkov radiation of the electron bunch with duration Δt_b moving through the slow-wave structure in the form of a periodically corrugated metallic waveguide. According to the Floquet theorem the electric field in the periodically corrugated waveguide can be presented as a sum of spatial harmonics:

$$\vec{E}(z,t) = \mathrm{Re}\left(A(z,t) \sum_{-\infty}^{+\infty} \vec{\tilde{E}}^{(n)}(\vec{r}_\perp) e^{i\omega t + in\bar{h}z + ihz} \right), \tag{1}$$

where ω is the carrier frequency, h is the longitudinal wave number of the fundamental harmonic, $\bar{h}=2\pi/d$, d is the period of the corrugation, $A(z,t)$ is the slow varied complex wave amplitude

$$\frac{1}{|A|}\frac{\partial |A|}{\omega\, \partial t} \ll 1, \quad \frac{1}{|A|}\frac{\partial |A|}{h\, \partial z} \ll 1,$$

and $\vec{\tilde{E}}^{(n)}$ is the transverse field profile of the spatial harmonics. In the case when the parameters of the corrugation (period or depth) are slightly tapered along the interaction space the amplitudes of the harmonics $\vec{\tilde{E}}^{(n)}$ should be slow functions of the longitudinal coordinate z.

Assuming that the magnetized electrons move in the axial direction only and interact with the single slow spatial harmonic $(n=-1)$ of the backward wave under synchronism condition (Fig. 1)

$$\omega = (-h + \bar{h}) V_0, \tag{2}$$

where $V_0=\beta_0 c$ is the unperturbed longitudinal velocity of the electrons. Neglecting the wave dispersion, the nonstationary excitation equation for the wave amplitude can be presented in the form [16]

$$\frac{\partial A}{\partial z} - \frac{1}{V_{gr}}\frac{\partial A}{\partial t} = f(t - z/V_0)\frac{\tilde{E}_z^{(-1)}(r_b,z)}{N} I_b J. \tag{3}$$

Here V_{gr} is the electromagnetic wave group velocity, I_b is the electron beam current, N is the norm of the operating waveguide mode, and $\tilde{E}_z^{(-1)}(r_b,z)$ is the longitudinal component of the synchronous spatial harmonic at the injection radius r_b of the hollow electron bunch. The function $f(t-z/V_0)$ describes the current profile of the electron bunch. The amplitude of the high-frequency (HF) electric current $J=1/\pi\int_0^{2\pi} e^{-i\theta} d\theta_0$ can be found from the equations of the electron motion

$$\left(\frac{\partial}{\partial z} + \frac{1}{V_0}\frac{\partial}{\partial t}\right)\gamma = -\frac{e}{mc^2}\,\mathrm{Re}[A(z,t)\tilde{E}_z^{(-1)} e^{i\theta}], \tag{4}$$

$$\left(\frac{\partial}{\partial z} + \frac{1}{V_0}\frac{\partial}{\partial t}\right)\theta = k\left[\frac{1}{\beta_\parallel} - \frac{1}{\beta_0}\right], \tag{5}$$

where $\theta=\omega(t-z/V_0)$ is the phase of an individual particle in the field of the synchronous harmonic, $\gamma=(1-\beta_\parallel^2)^{-1/2}$ is the relativistic mass factor.

Let us introduce the independent variables

$$\tau = \frac{\omega C(t - z/V_0)}{1 + V_0/|V_{gr}|}, \quad \zeta = \frac{\omega C z}{V_0},$$

where

$$C = \left(\frac{e I_b \hat{Z}}{2mc^2\gamma_0^3}\right)^{1/3} \ll 1$$

is the gain (Pierce) parameter, $\hat{Z} \equiv 2\langle \tilde{E}_z^{(-1)}(r_b)\rangle^2/k^2 N$ is the mean (along the interaction distance) coupling impedance of the tapered SWS with the full length l, $\langle \tilde{E}_z^{(-1)}(r_b)\rangle = (1/l)\int_0^l \tilde{E}_z^{(-1)}(r_b,z)dz$, $k=\omega/c$. In the new variables Eqs. (3)–(5) acquire the form

$$\frac{\partial a}{\partial \tau} - \frac{\partial a}{\partial \zeta} = \chi(\zeta) f(\tau) J, \tag{6}$$

$$\frac{\partial \gamma}{\partial \zeta} = -C\beta_0^3\gamma_0^3\,\mathrm{Re}[\chi(\zeta) a \exp(i\theta)], \tag{7}$$

$$\frac{\partial \theta}{\partial \zeta} = C\left[\frac{\beta_0}{\beta_\parallel} - 1\right], \tag{8}$$

where $a = eA\langle \tilde{E}_z^{(-1)}(r_b)\rangle/m\omega C^2\gamma_0^3 V_0$ is the dimensionless amplitude of the synchronous wave harmonic, the profile function $\chi(\zeta)$ describes the variation of the slow-wave structure parameters (first of all the corrugation depth). This function normalized as $(1/L)\int_0^L \chi(\zeta)d\zeta = 1$, where $L=\omega C l/V_0$ is the dimensionless length of the interaction space.

From Eq. (8) the longitudinal velocity can be expressed as

$$\beta = \frac{\beta_0}{1 + C\dfrac{\partial \theta}{\partial \zeta}}. \tag{9}$$

Taking into account Eq. (9) the motion equations acquire the form [13]

$$\frac{\partial^2\theta}{\partial\zeta^2} = \left\{\gamma_0^3\left[\left(1 + C\frac{\partial\theta}{\partial\zeta}\right)^2 - (1-\gamma_0^{-2})\right]^{3/2}\right\}\chi(\zeta)\mathrm{Re}[ae^{i\theta}]. \tag{10}$$

Under the assumption of $C \ll 1$ the variation of the electron longitudinal velocity in accordance with Eq. (9) is rather small and it is possible to simplify the motion equations (10)

$$\frac{\partial^2\theta}{\partial\zeta^2} = \left[1 + \nu\frac{\partial\theta}{\partial\zeta}\right]^{3/2}\chi(\zeta)\mathrm{Re}[ae^{i\theta}], \tag{11}$$

where $\nu = 2C\gamma_0^2$.

Below we assume that the electron density is constant $(f(\tau)=1, \tau \in [0,T])$ within a dimensionless bunch duration

$$\tau_b = \frac{\omega C}{1 + V_0/|V_{gr}|}\Delta t_b.$$

The development of SR emission is initiated by a small initial density perturbation at the system entrance, which is described by the parameter $\tilde{J}$. Under these assumptions the initial and boundary conditions for Eqs. (6) and (11) can be presented in the following form:

$$\theta|_{\zeta=0} = \theta_0 + \tilde{J}\cos\theta_0, \quad \theta_0 \in [0, 2\pi), \quad \left.\frac{\partial\theta}{\partial\zeta}\right|_{\zeta=0} = 0,$$

$$a(\tau, L) = 0, \quad a(0,\zeta) = 0. \tag{12}$$

Note that a self-consistent system of the equations (6) and (11) is written assuming a small pierce parameter $c \ll 1$ which justifies the use of the method of the slowly varying field amplitude. Obviously under such an assumption the radiation spectrum width $(\Delta\omega \sim C\omega)$ is sufficiently narrow in the scale of the finite passband of the slow-wave structure and it is possible to neglect the wave dispersion. It is also important to emphasize that for the relativistic electrons in spite of the assumption of a small variation of velocities as used in Eq. (11), the variation of the kinetic energy can be rather large.

A. Superradiance in the uniform slow-wave structure

The stimulated emission of an electron bunch of finite duration in the backward propagating electromagnetic wave has been studied by numerical simulations of Eqs. (6) and (11). The evolution of field intensity inside the interaction space for the electron bunch of total duration $\tau_b = 8$ moving in the uniform slow-wave structure $[\chi(\zeta)=1]$ is shown in Fig. 2. At the output of the interaction space $\zeta=0$ the radiation represents a short pulse (Fig. 3, curve 1). The formation of the short pulse of the superradiance involves the electrons self-bunching and the mutual influence of different electron fractions due to the propagation of the wave along the electron bunch with a group velocity having the opposite direction with respect to the electron longitudinal velocity. The SR pulse duration may be estimated as $\Delta t_{SR} \sim |\mathrm{Im}\ \omega|^{-1}$, where Im ω is the instability gain, which in the asymptotical case when $L \to \infty$ tends to

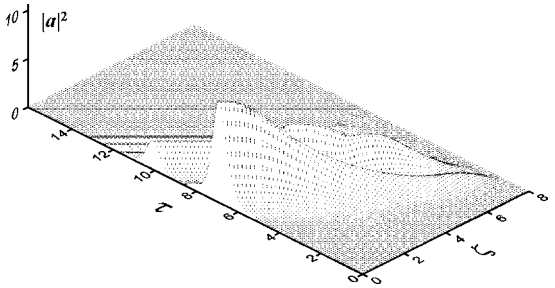

FIG. 2. Formation of a short superradiance pulse in the uniform slow-wave structure. $(L=8,\ \tau_b=8,\ \nu=0.5,\ \tilde{J}=0.01)$.

$$|\mathrm{Im}\ \omega| = \frac{3^{3/2}2^{1/3}}{4}\frac{C\omega}{1 + V_0/V_{gr}}.$$

The distinctive feature of superradiance [17] is the square dependence of the radiation power on the total number of electrons in the bunch N. To confirm this fact the dependence of the SR pulse amplitude on the electron pulse duration is presented in Fig. 4(a) for the case of a constant beam current $(\nu=0.5)$ and different parameters of initial modulation $\tilde{J}$. The peak amplitude is proportional to the electron pulse duration until its duration is rather short: $\tau_b < 6$. Correspondingly the radiation peak power is proportional to N^2. It should be noted that the effective SR pulse duration decreases with increasing amplitude [see Fig. 4(b)], which is also a feature typical of the superradiance [17]. Saturation of the growth of the peak amplitude occurs when the electron pulse duration exceeds a certain value $\tau_b > 6$, and the electron beam becomes too long to provide coherent radiation from all particles over the total beam length. For a rather long electron bunch the "multi-spiked" generation regime is realized, because different parts of the bunch radiate practically independently (Fig. 5). In the case of the backward wave interaction such a regime is similar to the self-modulation regime in the backwave oscillators (BWO) driven by a quasistationary electron beam [16]. The curve 2 in Fig. 4(a) corresponds to the larger initial modulation of the electrons density $\tilde{J}$. In this case the saturation occurs for a shorter electron bunch and the SR pulse peak

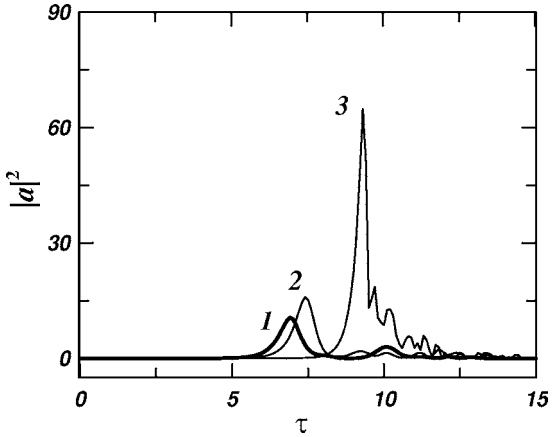

FIG. 3. Superradiance pulses at the interaction space output $\zeta = 0$: (1) in the uniform SWS, (2) in the nonuniform SWS with linear increasing profile function $\chi(\zeta)$, (3) in the optimized nonuniform SWS with the profile function given by Eq. (14).

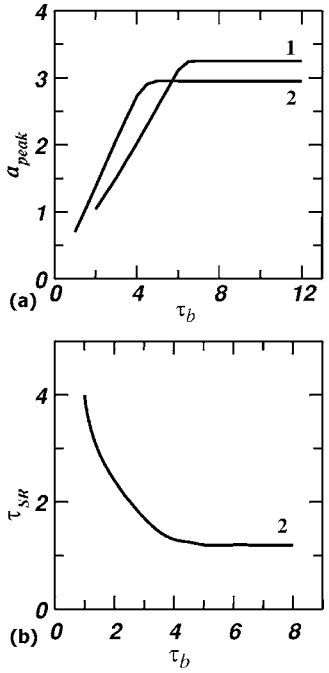

FIG. 4. Dependence of the SR pulse peak amplitude (a) and pulse width (b) on the electron pulse duration for the fixed beam current (L=8, τ_b=8, ν=0.5):1, J=0.01; 2, J=0.1.

amplitude achieves a smaller value. Therefore for a fixed length of the interaction space $L \gg 1$ thereis an optimal value of the initial modulation $\tilde{J}_{\text{opt}} \sim \exp(-L)$. In this case the amplitude of the HF current saturates due to a nonlinearity just near the SWS collector edge. Under such conditions the SR pulse arrives at the output cross section $\zeta=0$ at $\tau_\Sigma \approx L$ (Fig. 2). It means that time for the SR pulse extraction is approximately equal to the sum of the time it takes for the particle and the wave to pass through the interaction space. In this case the SR pulse forming at the initial stage of the interaction accumulates energy from the electron bunch with total duration

$$\Delta t_\Sigma = l\left(\frac{1}{V_\parallel} + \frac{1}{V_{gr}}\right).$$

If, with a given value of L, the perturbation amplitude $\tilde{J}$ exceeds the optimum value, the SR pulse is formed earlier, but with a lower peak power (the HF current saturates earlier than the time it takes for the particles to pass through the SWS). Conversely, if the initial noise is too small, the interaction distance should be increased to obtain a SR pulse with the same peak amplitude.

It is important to note that the SR pulse peak power can exceed the power of the driving electron bunch because a short SR pulse that forms at the initial stage of the interaction can accumulate energy from different fractions of an extended electron bunch. Nevertheless, in accordance with the energy conservation law, the SR pulse total electromagnetic energy is smaller than the beam kinetic energy. The necessary condition for the realization of such a regime is that the SR pulse duration is much shorter than the energy accumulation time $\Delta t_{SR} \ll \Delta t_\Sigma$.

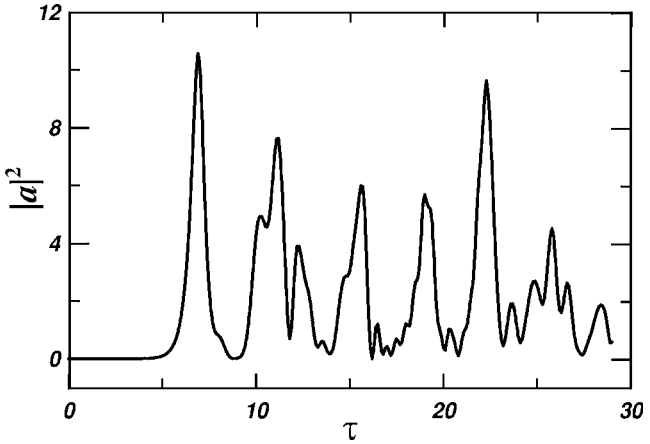

FIG. 5. "Multispiked" generation regime in the case of the long electron bunch: τ_b=40.

It is convenient to introduce the power conversion factor (coefficient) as a ratio of the SR pulse peak power $P_{\max}$ and the electron beam power

$$K = \frac{eP_{\max}}{I_b mc^2(\gamma_0 - 1)}.$$

In designations used in Eqs. (6) and (11) the conversion factor can be presented in the form [13]

$$K = \frac{(\gamma_0 + 1)}{\gamma_0} F(\nu), \quad F(\nu) \equiv \frac{\nu |a(\tau,0)|^2_{\max}}{8}. \tag{13}$$

Function $F(\nu)$ for the uniform slow-wave structure of fixed length L=8 is presented in Fig. 6. With increasing of the interaction distance L the maximum value of $F(\nu)$ increases and tends to unity for the $L \to \infty$. Thus, for ultrarelativistic electrons with $\gamma_0 \gg 1$ the conversion coefficient K does not exceed a factor of one. With decreasing the electrons energy the conversion coefficient rises due to the term $(\gamma_0+1)/\gamma_0$ in expression (13). For a moderately relativistic electron beam, i.e., electron energies are about 250–300 keV (γ_0=1.4–1.6), a conversion coefficient can exceed unity. For example, for L=8 the conversion coefficient amounts to $K \sim 1.2$. The direct simulations of full Eqs. (6) and (10) also demonstrate the possibility of achieving a conversion factor of $K>1$ [13].

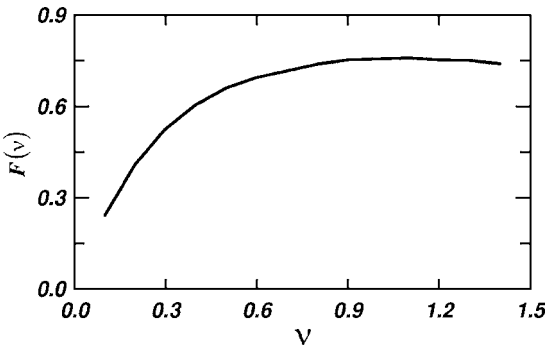

FIG. 6. Function $F(\nu)$ for the uniform slow-wave structure of the fixed length L=8.

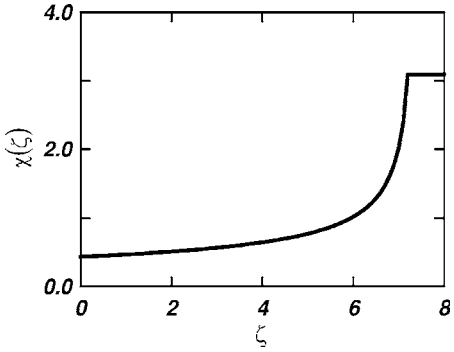

FIG. 7. The profile function $\chi(\zeta)$ providing the constant amplitude of the acting field along the interaction space.

B. Superradiance in the nonuniform slow-wave structure

To achieve a more substantial excess of the SR pulse peak power over the power of electron bunch it is feasible to use a nonuniform slow-wave structure with variable coupling impedance. As suggested in Ref. [13] the coupling impedance should decrease at the cathode end. In this case the SR pulse propagating towards the cathode will intersect characteristics of electron fractions with rather small modulation and will extract energy from these fractions. For example, it is possible to use a slow-wave structure with a corrugation depth and, correspondingly, function $\chi(\zeta)$, which is linearly increasing from the cathode end. Curve 2 in Fig. 3 shows the SR pulse in the case when the corrugation depth is increased to a factor of 1.6 along the first half of the SWS length. In the simulations, when $L=8$ and $\gamma_0=1.6$, the conversion factor amounts to 1.7. A slow-wave structure with such a tapering has been used successfully in the experiments described in Sec. III, where SR pulses with a peak power exceeding the power of the driving beam have been generated.

Further increasing of the power conversion factor can be achieved by more sophisticated profiling of the corrugation depth. It is beneficial to realize a situation when despite a linearly growing peak power of the microwave pulse $|a(\tau,\zeta)|^2$ the electric field strength of the synchronous harmonic acting on the electrons $|\chi(\zeta)a(\tau,\zeta)|$ is constant, as the electron bunch propagates through the system. The profile function $\chi(\zeta)$ satisfying the above condition may be presented in the form (Fig. 7)

$$\chi(\zeta)=\begin{cases}\dfrac{\chi_0}{\left[p_0-(p_0-1)\dfrac{\zeta}{\zeta_0}\right]^{1/2}} & \text{if } 0\le\zeta\le\zeta_0\\ \chi_0 & \text{if } \zeta_0\le\zeta\le L,\end{cases}\qquad(14)$$

where the parameter p_0 defines the relative impedance variation. The process of the SR pulse formation in the case of a tapered coupling impedance (14) for $p_0=50$ and $\zeta_0=0.93L$ is presented in Fig. 8(a). In accordance with the above assumptions the amplitude of the synchronous space harmonic $|\chi(\zeta)a(\tau,\zeta)|$ in the nonlinear stage of the interaction practically stays constant as it is seen from Fig. 8(b). For the situation considered a maximum conversion factor of $K\sim4$ may be achieved. Thus the implementation of a nonuniform

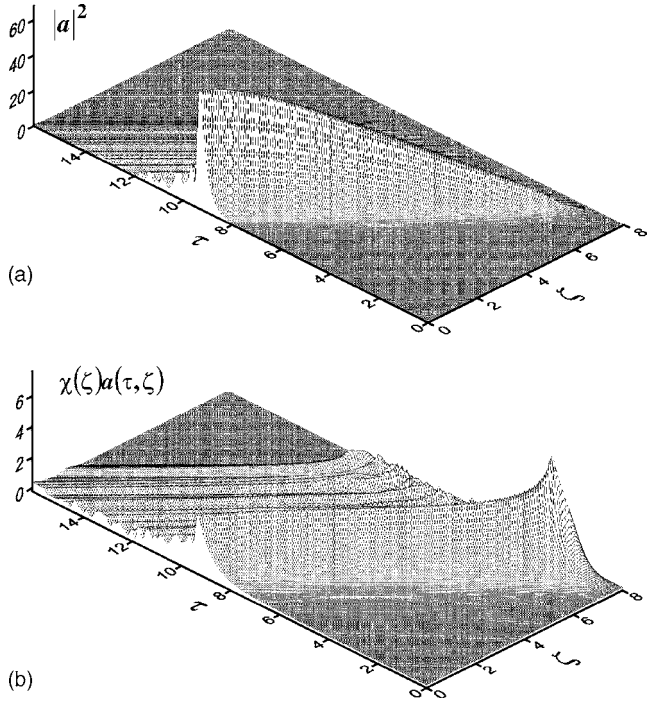

FIG. 8. (a) Formation of the SR pulse in the optimized nonuniform SWS with the peak power exceeding the electron bunch power ($K>4$). (b) The amplitude of the synchronous space harmonic.

SWS profile allows the SR pulse peak power to be increased substantially. For comparison with the previous cases (uniform SWS and SWS with linear increasing impedance) the output SR pulse profile is presented by curve 3 in Fig. 3.

Nevertheless there are a number of effects that can decrease the conversion coefficient which are not taken into account in the theoretical model described above. These effects include the group velocity dispersion, interaction with the nonsynchronous harmonics, and the space charge effects and influence of the guiding magnetic field. In particular, the diversity $\Delta V_\parallel$ of the electron velocities of the beam formed in the low magnetic field can result in the bunching destruction and for highly efficient processes the condition $\Delta V_\parallel t_{SR}\ll\lambda$ should be applied. To include these factors additional PIC simulations based on the axial symmetric version of the KARAT code [18] have been carried out. The PIC code allows integrating directly (without averaging) Maxwell equations together with the electron motion equations in the real geometry of the interaction space. In Sec. III we describe both the experimental results and PIC code simulations with satisfactory agreement demonstrated.

III. PIC CODE SIMULATIONS AND THE FIRST EXPERIMENTS ON PRODUCTION OF SR PULSES WITH PEAK POWER EXCEEDING THE POWER OF ELECTRON BEAM

Taking into account the theoretical consideration, in the nonuniform SWS it is possible to generate electromagnetic SR pulses with peak power substantially exceeding the power of the driving electron beam (conversion factor K

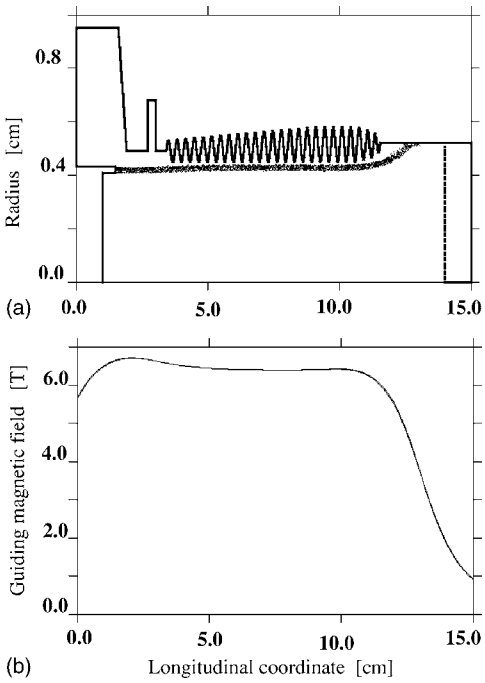

FIG. 9. (a) The geometry of the experimental setup with nonuniform SWS used in KARAT simulations and (b) the profile of the magnetic field that provides the additional tapering of the SWS and prevents the fall of electrons on the waveguide wall.

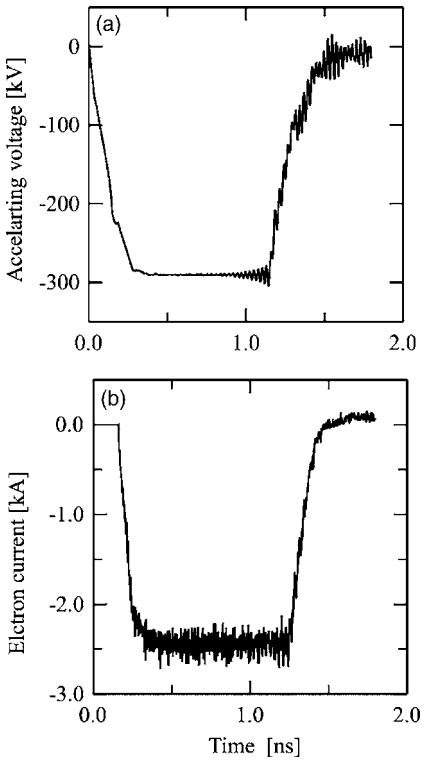

FIG. 10. The acceleration voltage pulse profile (a) and the corresponding current pulse (b) used in the KARAT PIC code simulations of the Ka-band experiment.

>1). This fact was confirmed experimentally. SR pulses with a conversion factor $K \approx 1.4-1.8$ were obtained in the Ka- and X-frequency bands. In the experiments the slow-wave structures with a linear increase of the coupling impedance along the first half of the length of the interaction region have been used. At the beginning of each experiment simulation using the axial symmetric version of the PIC code KARAT were carried out the main purpose being to optimize the parameters of the nonuniform SWS. As a result in the Ka- and X-band frequency range ultrashort SR pulses with a peak power over 1 GW were produced.

A. Ka band

The geometry of the Ka-band experimental setup used in the KARAT simulations is presented in Fig. 9(a). To diminish the dispersion expansion of the SR pulse during its propagation along the slow wave structure slightly oversized SWS with $D/\lambda=1.3$ and a resonant reflector for extraction of the electromagnetic pulse from the interaction space were used. The optimized SWS has a length of about 12 cm ($\sim 14\lambda$) and a period of corrugation of 0.33 cm. The amplitude of the corrugation was increased from 0.03 to 0.065 cm along the first half of the system. Additional tapering of the coupling impedance was provided by a special profile of the magnetic field increasing the gap between the electron beam and SWS at the cathode end [Fig. 9(b)]. Such profiling also prevented the intersection of the electrons on the wall of the microwave system due to the action of the SR pulse field, which was strong enough at the cathode region to affect the large transverse oscillations.

Along with the simulations of the radiation processes the numerical model includes the formation of the electron bunch in the coaxial vacuum diode based on the self-consistent electron emission model. In the modeling the value of the electron current pulse and its profile in the interaction space was determined by the geometry of the electron gun and driving voltage pulse. For a voltage pulse of 1 ns duration and amplitude of 290 kV [Fig. 10(a)] the corresponding current pulse [Fig. 10(b)] had a peak current of ~ 2.5 kA that coincided well with the experimental measurements. The respective power of the electron bunch was ~ 700 MW. In accordance with the simulations in the strong magnetic field of up to 6.5 T the electron bunch with such power can emit a 200 ps SR pulse with a peak power of up to 1.2 GW (Fig. 11). As a result the conversion factor achieved was 1.7.

At the Ka band the experiments have been performed based on the RADAN-303BP accelerator, which can provide 1 ns 270–290 kV accelerating voltage pulses [19]. In these experiments the SR pulses with parameters close to the values found from the simulations were obtained. The typical oscilloscope trace of a Ka-band SR pulse is presented in Fig. 12. The peak power of the SR pulse was ~ 1 GW which corresponds to a conversion factor of ~ 1.4 [15].

B. X band

The maximum conversion factor of the SR pulses was achieved in the experiments at the X band. The first experiment employed the SINUS-150 compact electron accelerator,

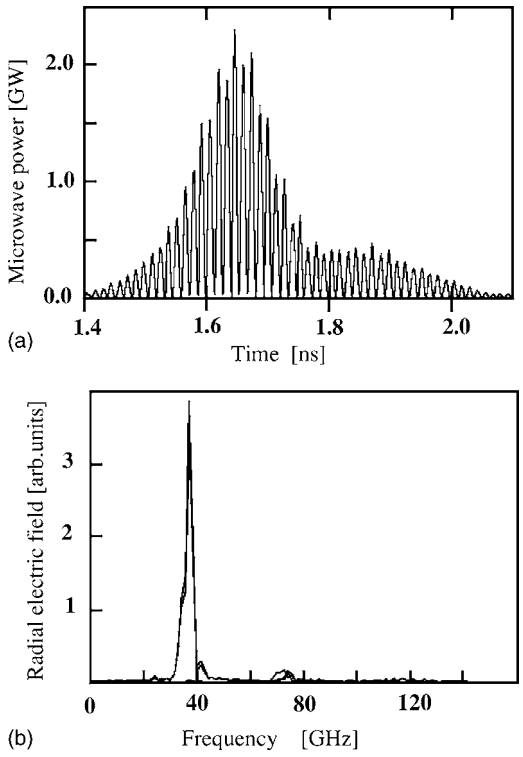

FIG. 11. (a) The Ka-band SR pulse and (b) its spectrum given by KARAT simulations.

which provided electron pulses of 4 ns duration [20]. The diode voltage was varied from 230 to 330 kV. Correspondently with the diode geometry used the beam current changed from 1.6 to 2.6 kA. Thus, the maximum power of the electron beam was 0.9 GW. An annular electron beam with an external diameter of 3.4 cm passed through the SWS in the uniform axial magnetic field of 3 T generated by the pulsed solenoid. The slow-wave structure had a mean radius 1.9 cm, period of the corrugation of 1.3 cm, and was 22 periods in length. The amplitude of the corrugation was increased from 0.14 to 0.23 cm along the system. The conversion factor predicted by the KARAT simulations in such a system was found to be 1.5.

For the experiment carried out, the shape of the microwave detector signals recorded by the digital oscilloscope with a 3-GHz analog bandwidth is shown in Fig. 13(a). The microwave pulse energy measured with a calorimeter reached 0.6 J; taking into account the pulse width this corresponds to a peak power of 1.2 GW [14]. Thus the power

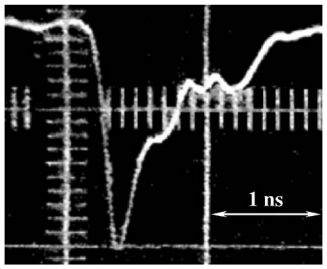

FIG. 12. Oscilloscope trace of 1 GW, 200 ps Ka-band SR pulse.

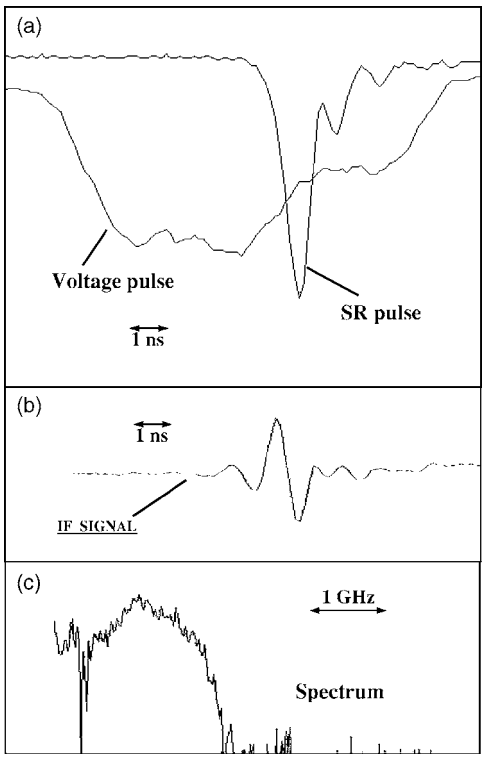

FIG. 13. (a) Oscilloscope traces of voltage pulse and 1.2 GW X-band SR pulse. (b) Intermediate frequency (IF) signal after heterodyning. (c) Spectrum of X-band SR pulse. The heterodyne frequency is 8.4 GHz.

conversion coefficient was estimated to be 1.4, which is in a good agreement with the results of simulations presented above. The SR pulse spectrum [Fig. 13(b)] measurement was performed using a heterodyne technique. The central frequency of the SR pulse was 9.3 GHz with 7–15% width, which is close to the natural one expected at the (−3) dB level.

Further increase of the conversion factor was obtained in the next X-band experiment [14]. A peculiarity of this experiment was the extraction of the electromagnetic pulse directly from the cathode end. As a result the influence of the dispersion was diminished since the electromagnetic pulse does not propagate through the SWS in the forward direction. This experiment was performed using the SINUS-200 compact accelerator [21] forming the electron beam with a current of 5 kA and a particle energy of 330 keV, corresponding to a beam power ~1.7 GW. The peak power of the SR pulse with the duration of 0.65 ns was ~3 GW which corresponds to a conversion factor of 1.8.

IV. SUMMARY

The general analysis of the superradiance was carried out for the interaction of an extended electron bunch with the backward wave propagating in the slow wave structure. It is shown that the radiation of such an electron bunch has some features, which are specific for the superradiance, including the quadratic dependence of the radiation peak power on the

total number of the electrons and the decreasing of an effective SR pulse width with an increasing number of the electrons. The conditions have been found when the peak power of the SR pulse could exceed the driving electron beam power (power conversion factor exceeds 1). It is caused by the effect of the energy accumulation in the process of the propagation of a short SR pulse through the electron beam. The optimization of the impedance profile of the slow wave structure allows increasing the conversion factor by several times in comparison with the uniform SWS.

The results of the theoretical consideration are confirmed by the experimental studies of superradiance emission and direct PIC code simulations. The SR pulses observed with the SINUS-150 accelerator (electron pulse width 4 ns, voltage 330 kV, beam current 2.6 kA) at the X band have the following parameters: duration of 0.6–0.8 ns and a peak power of 1.2 GW (the conversion factor 1.5). Similarly Ka-band experiments based on the RADAN-303BP accelerator (pulse width 1 ns, voltage 290 kV, beam current 2.5 kA) produced SR pulses with a duration of 200 ps and a peak power of 1 GW (the conversion factor 1.4).

The progress that has been achieved in this research has enabled a type of microwave generator to be created capable of producing unique short electromagnetic pulses (200–300 ps at the Ka band and 600–800 ps at the X band) with superhigh peak powers in excess of 1 GW. A further important achievement based on the above results is the realization of sources of SR pulses operating at a high repetition frequency rate. At the Ka band a pulse repetition frequency rate of 3.5 kHz with an average microwave power, over the train of 300 MW pulses, was 200 W. A superradiative X-band source [22] operating in the burst-repetitive mode (1 s; ~700 Hz) generated an average power of microwave radiation of up to 2.5 kW when the peak power of SR pulses exceeded 2 GW. These sources of powerful ultrashort microwave pulses may find application in radar systems with high spatial resolution, in electromagnetic compatibility testing, as well as in biomedical experiments.

ACKNOWLEDGMENTS

This work was supported in part by Russian Foundation for Basic Research under Grants No. 05-02-08016, No. 05-02-17510, and No. 05-02-08240. The authors are grateful to Dr. A. Cross for useful discussions and help in manuscript preparation.

[1] N. S. Ginzburg, I. V. Zotova, and A. S. Sergeev, Tech. Phys. Lett. **25**, 25 (1999).
[2] R. Bonifacio, C. Maroli, and N. Piovella, Opt. Commun. **68**, 369 (1988).
[3] R. Bonifacio, B. W. J. McNeil, and P. Pierini, Phys. Rev. A **40**, 4467 (1989).
[4] R. Bonifacio, N. Piovella, and B. W. J. McNeil, Phys. Rev. A **44**, R3441 (1991).
[5] N. S. Ginzburg, Sov. Tech. Phys. Lett. **14**, 197 (1988).
[6] N. S. Ginzburg, I. V. Zotova, and A. S. Sergeev, Pis'ma Zh. Tekh. Fiz. **60**, 501 (1994).
[7] N. S. Ginzburg, Yu. V. Novozhilova, and A. S. Sergeev, Tech. Phys. Lett. **22**, 359 (1996).
[8] G. R. M. Robb, N. S. Ginzburg, A. D. R. Phelps, and A. S. Sergeev, Phys. Rev. Lett. **77**, 1496 (1996).
[9] D. A. Jaroszynski, P. Chaix, and N. Piovella, Phys. Rev. Lett. **78**, 1699 (1997).
[10] N. S. Ginzburg, A. S. Sergeev, I. V. Zotova, A. D. R. Phelps, A. W. Cross, V. G. Shpak, M. I. Yalandin, S. A. Shunailov, and M. R. Ulmaskulov, Phys. Rev. Lett. **78**, 2365 (1997).
[11] N. S. Ginzburg, A. S. Sergeev, I. V. Zotova, Yu. V. Novozhilova, R. M. Rozental, A. D. R. Phelps, A. W. Cross, V. G. Shpak, M. I. Yalandin, S. A. Shunailov, and M. R. Ulmaskulov, Opt. Commun. **175**, 139 (2000).
[12] N. S. Ginzburg, I. V. Zotova, Yu. V. Novozhilova, A. S. Sergeev, N. Yu. Peskov, A. D. R. Phelps, A. W. Cross, K. Ronald, G. Shpak, M. I. Yalandin, S. A. Shunailov, M. R. Ulmaskulov, and V. P. Tarakanov, Phys. Rev. E **60**, 3297 (1999).
[13] A. A. Elthaninov, S. D. Korovin, V. V. Rostov, I. V. Pegel, G. A. Mesyats, M. I. Yalandin, and N. S. Ginzburg, Pis'ma Zh. Tekh. Fiz. **77**, 314 (2003).
[14] A. A. Elthaninov, S. D. Korovin, V. V. Rostov, I. V. Pegel, G. A. Mesyats, S. N. Rukin, V. G. Shpak, M. I. Yalandin, and N. S. Ginzburg, Laser Part. Beams **21**, 187 (2003).
[15] S. D. Korovin, G. A. Mesyats, V. V. Rostov, M. R. Ulmaskulov, K. A. Sharypov, V. G. Shpak, S. A. Shunailov, and M. I. Yalandin, Pis'ma Zh. Tekh. Fiz. **30**, 68 (2004).
[16] N. S. Ginzburg, S. P. Kuznetsov, and T. M. Fedoseeva, Radiophys. Quantum Electron. **21**, 729 (1979).
[17] J. C. MacGillivray and M. S. Feld, Phys. Rev. A **14**, 1169 (1976).
[18] V. P. Tarakanov, *User's Manual for Code KARAT* (Berkeley Research Associates, Springfield, 1992).
[19] G. A. Mesyats, S. D. Korovin, V. V. Rostov, V. G. Shpak, and M. I. Yalandin, Proc. IEEE **92**, 1166 (2004).
[20] V. P. Gubanov, S. D. Korovin, I. V. Pegel, A. M. Roitman, V. V. Rostov, and A. S. Stepchenko, IEEE Trans. Plasma Sci. **25**, 258 (1997).
[21] V. P. Gubanov, A. V. Gunin, S. D. Korovin, and A. S. Stepchenko, Prib. Tekh. Eksp. **1**, 73 (2002).
[22] S. K. Luybutin, S. N. Rukin, K. A. Sharypov, V. G. Shpak, S. A. Shunailov, B. G. Slovikovsky, M. R. Ulmaskulov, M. I. Yalandin, S. D. Korovin, and V. V. Rostov, IEEE Trans. Plasma Sci. **33**, 1220 (2005).